

## EMANATION THERMAL ANALYSIS OF NATURAL AND CHEMICALLY-MODIFIED VERMICULITE

J. POYATO<sup>1,\*</sup>, L. A. PÉREZ-MAQUEDA<sup>1</sup>, A. JUSTO<sup>1</sup> AND V. BALEK<sup>2</sup>

<sup>1</sup> Instituto de Ciencia de Materiales de Sevilla, CSIC-University of Seville, c/ Américo Vespucio, s/n 41092 Sevilla, Spain

<sup>2</sup> Institute of Inorganic Chemistry AS CR, 250 68 Řež, Czech Republic

**Abstract**—Emanation thermal analysis (ETA), based on radon release measurements from previously labeled samples, was used for the first time in the characterization of the thermal behavior of natural Mg<sup>2+</sup>-vermiculite (Santa Olalla, Huelva, Spain) and of Na<sup>+</sup>- and NH<sub>4</sub><sup>+</sup>-exchanged vermiculite samples. In addition, vermiculite samples subjected to a chemical treatment with an aqueous solution of (NH<sub>4</sub>)<sub>2</sub>SiF<sub>6</sub> and partially or totally re-saturated with Na<sup>+</sup> ions were also investigated by ETA. The ETA results of natural Mg<sup>2+</sup>-vermiculite, Na<sup>+</sup>-vermiculite and NH<sub>4</sub><sup>+</sup>-vermiculite gave supplementary information about microstructure changes of the samples observed under dynamic heating conditions. The method has proved to be very useful for characterization of microstructure changes due to modification in the interlayer space of samples during the heat treatment. The crystallization of vermiculite into new phases, such as enstatite (for NH<sub>4</sub><sup>+</sup>-vermiculite and Mg<sup>2+</sup>-vermiculite) and forsterite (for Na<sup>+</sup>-vermiculite) was also observed by ETA.

**Key Words**—DTA, Emanation Thermal Analysis, Interlayer Space, Microstructure, Thermogravimetry, Vermiculite.

### INTRODUCTION

Negative charge in vermiculite due to substitutions in tetrahedral and octahedral sheets is compensated by the cations in the interlayer space. Cation exchange in the interlayer causes changes not only in the interlayer space, but also in the thermal behavior of the vermiculite. Additionally, phyllosilicates can be chemically modified by exchanging the tetrahedral Si<sup>4+</sup> for Al<sup>3+</sup> with (NH<sub>4</sub>)<sub>2</sub>SiF<sub>6</sub> (Miyake *et al.*, 1987). This method, originally applied to zeolites (Breck *et al.*, 1985), has been used in vermiculites for (1) reduction of the net negative charge in vermiculites by substitution of Si<sup>4+</sup> for Al<sup>3+</sup> in the tetrahedral sheet; and (2) pillaring of the negative-charge depleted vermiculite with the cation Al<sub>13</sub>O<sub>4</sub>(OH)<sub>24</sub>(H<sub>2</sub>O)<sub>7</sub><sub>12</sub><sup>7+</sup> (d'Espinose de la Caillerie and Fripiat, 1991).

Thermal evolution of vermiculite samples is very much affected by the cation in the interlayer space and by the chemical treatment of the samples. To follow the thermal evolution, different thermal analysis methods are available. Weight loss and heat flow could be registered as a function of temperature by conventional methods. The thermal analysis of clay minerals by conventional methods has been studied extensively. A relatively new and unconventional method is now available, emanation thermal analysis (ETA), which enables users to follow the thermal evolution of samples by measuring the release of the inert radioactive radon gas from solid samples previously labeled with the radionuclides <sup>228</sup>Th and <sup>224</sup>Ra compounds (Balek, 1989, 1991; Balek and Tölgyessy, 1984). Some of the radon

(<sup>220</sup>Rn) atoms formed by spontaneous  $\alpha$ -decay of radium <sup>224</sup>Ra are trapped in the structural defects, such as vacancy clusters, grain boundaries and pores, and can be released from the sample by diffusion. Thus, the defects in the solids serve both as traps and diffusion paths for radon. Consequently, changes in the particle size, surface area, pore structure, number of point defects and other large-scale defects referred to in general as microstructural changes, can be monitored by means of ETA under dynamic conditions of heating. The ETA curves should be analyzed in terms of increases and decreases in the radon emanation rate as a function of temperature. Thus, an increase in the emanation rate indicates that new paths are open for the release of the trapped radon. On the other hand, a decrease in the radon emanation rate indicates that the release of radon is hindered due to a change in the structure or microstructure of the sample.

Emanation thermal analysis is a very sensitive method. Thermal processes where no weight loss takes place or the enthalpy of the reaction is very low and, therefore, cannot be detected by conventional thermogravimetry or differential thermal analysis (DTA) (or calorimetry), can be detected by ETA if the process produces a microstructural modification that changes the emanation of radon. For example, the evolution of porosity in hematite with temperature has been studied by ETA while no other thermal method was sensitive to such changes (Pérez-Maqueda *et al.*, 2002). For phyllosilicates, ETA is a very promising analytical method, because it gives information about the interlayer space (Málek *et al.*, 1997; Balek *et al.*, 1998, 1999). During impregnation, <sup>228</sup>Th and <sup>224</sup>Ra are incorporated into the interlayer and, in the subsequent heating, radon emanation

\* E-mail address of corresponding author: jpoyato@us.es

tion gives an indication of the diffusion of the radon in the interlayer space towards the exterior. In addition, some Rn could be adsorbed on edges or cracks, and its diffusion gives information on the vermiculite surface. Moreover, some of the radon gets into the structure by diffusion and emanates at high temperatures indicating structural or microstructural transformation of the material.

The objective of this paper is to explore the possibilities of the unconventional emanation thermal analysis methods for the characterization of the thermal behavior of a natural  $\text{Mg}^{2+}$ -vermiculite sample before and after ion exchange reactions with  $\text{Na}^+$  and  $\text{NH}_4^+$  and after chemical treatment with ammonium hexafluorosilicate. Special attention is paid to the study of the microstructural changes during thermal treatment. The ETA results are compared with the results obtained from more conventional methods, such as thermogravimetry (TG), DTA, powder X-ray diffraction (XRD) and infrared (IR) spectroscopy.

## EXPERIMENTAL

### Materials

The vermiculite from Santa Olalla (Huelva, Spain) was used as a starting material (González García and García Ramos, 1961; Justo, 1984). Its half unit-cell composition is  $\text{Mg}_{0.439}(\text{Si}_{2.64}\text{Al}_{1.36})(\text{Mg}_{2.48}\text{Fe}_{0.324}^{3+}\text{Fe}_{0.036}^{2+}\text{Al}_{0.14}\text{Ti}_{0.01})\text{O}_{10}(\text{OH})_2$  (Pérez-Maqueda *et al.*, 2001). Large flakes were ground using a Knife-mill (Netzsch ZSM-1, Germany) and sieved. Vermiculite particles  $<80 \mu\text{m}$  in size were used for the experiments. This sample is hereafter referred to as  $\text{Mg}^{2+}$ -V.

The  $\text{Na}^+$ -saturated sample ( $\text{Na}^+$ -V) was prepared from the natural  $\text{Mg}^{2+}$ -vermiculite by repeated contact with a 1 M NaCl solution, under stirring, at room temperature. The sample was washed with distilled water until the supernatant solution became free of  $\text{Cl}^-$ . The  $\text{NH}_4^+$ -saturated vermiculite ( $\text{NH}_4^+$ -V) was prepared from the  $\text{Na}^+$ -vermiculite by repeated contact with a 1 M ammonium acetate solution ( $\text{pH} = 7$ ) at room temperature. The excess of ammonium acetate was subsequently washed out with distilled water and the slurry was separated by centrifugation. The presence of the  $\text{NH}_4^+$ -vermiculite was confirmed by XRD ( $d_{001} = 10.5 \text{ \AA}$ ; MacEwan and Wilson, 1980).

The  $\text{Na}^+$ -V sample was treated with  $(\text{NH}_4)_2\text{SiF}_6$  according to the procedure described by d'Espinose de la Caillerie and Fripiat (1991): 0.5 g of  $\text{Na}^+$ -V were suspended in 100 mL of a 1 M ammonium acetate buffer solution ( $\text{pH} = 7.8$ ) and an aqueous solution of  $(\text{NH}_4)_2\text{SiF}_6$  was added dropwise ( $\sim 10$  drops/min) to the stirred suspension at  $\sim 60^\circ\text{C}$  to reach an atomic ratio (Si added/Al(IV) in vermiculite; Al(IV) means  $\text{Al}^{3+}$  in tetrahedral coordination) equal to 0.75; after the addition of  $(\text{NH}_4)_2\text{SiF}_6$  the overall reaction time (at  $\sim 60^\circ\text{C}$ ) was 2 days. After cooling, the suspension was centrifuged,

the supernatant solution removed and the remaining solid was washed 10 times with distilled warm ( $\sim 70^\circ\text{C}$ ) water.

During this treatment the  $\text{Na}^+$  could have been exchanged by  $\text{NH}_4^+$  ions. In order to retain the  $\text{Na}^+$  saturation, the sample was treated three times with 15 mL of 1 M NaCl solution under stirring at room temperature over a period of 24 h. After treatment with the NaCl solution, the samples were washed with distilled water until the solution was free of  $\text{Cl}^-$  ions. The XRD patterns indicated the presence of both  $\text{Na}^+$ - and  $\text{NH}_4^+$ -vermiculite, ( $d_{001} \approx 12$  and  $10.5 \text{ \AA}$ , respectively; relative humidity  $\approx 50\%$ ; henceforth called  $\text{NH}_4^+$ / $\text{Na}^+$ - $\text{V}_{\text{dealum}}$ ). Therefore we repeated this procedure a few times more until the presence of the  $\text{Na}^+$  ions alone in the interlayer space was confirmed by XRD ( $d_{001} \approx 12 \text{ \AA}$ , relative humidity  $\approx 50\%$ ; MacEwan and Wilson, 1980). This sample is referred to as  $\text{Na}^+$ - $\text{V}_{\text{dealum}}$ .

All vermiculite samples were dried in air at room temperature prior to their characterization.

### Methods used for sample characterization

Emanation thermal analysis (Balek, 1991; Balek and Tölgyessy, 1984; Balek *et al.*, 2002) involves the measurements of radon release rate from samples previously labeled. The samples for ETA were labeled by soaking with acetone solution containing traces of  $^{228}\text{Th}$  and  $^{224}\text{Ra}$  nitrates. The specific activity of a sample after labeling was  $10^5 \text{ Bq/g}$ . Atoms of  $^{220}\text{Rn}$  were formed by the spontaneous  $\alpha$  decay of  $^{228}\text{Th}$  and  $^{224}\text{Ra}$ . The  $^{224}\text{Ra}$  and  $^{220}\text{Rn}$  atoms were incorporated into the sample to a maximum depth of 80 nm due to the recoil energy (85 keV/atom), which the atoms gain by the spontaneous  $\alpha$  decay. The maximum depth of  $^{220}\text{Rn}$  penetration was 80 nm as calculated with the TRIM code (Ziegler *et al.*, 1985).

The ETA-DTA measurements were performed on samples in a flow of dry air at a heating rate of 6 K/min, using a modified NETZSCH DTA 404 instrument. During the ETA-DTA measurements the labeled sample (0.1 g) was placed in a corundum crucible with a constant overflow of dry air (flow rate 40 mL/min), which carried the radon released from the sample into the measuring chamber of radon radioactivity. Details of the ETA measurements and data treatment have been described elsewhere (Balek, 1989, 1991).

Thermogravimetric measurements were carried out in the same experimental conditions as the ETA-DTA measurements using a Setaram 2000 apparatus. X-ray powder diffraction patterns of basal oriented samples were obtained by means of a 5000 SIEMENS powder XRD unit using monochromated  $\text{CuK}\alpha$  radiation. High-temperature X-ray powder diffraction experiments were performed on a Philips (X'Pert) diffractometer with a high-temperature chamber (HTK 1200, Anton Paar) using Ni-filtered  $\text{CuK}\alpha$  radiation and a position-sensitive detector (ASA-S, MBraun). For the heating we used

identical conditions to those used for the other thermal analysis measurements. Infrared spectra were obtained on pellets of 2 cm diameter, prepared by mixing 3 mg of sample with 300 mg of KBr and using the FTIR Spectrometer NICOLET, Type 510.

## RESULTS AND DISCUSSION

### *Thermal behavior of $Mg^{2+}$ -, $Na^+$ - and $NH_4^+$ -vermiculites in the range 25–300°C*

Results of the ETA of the natural  $Mg^{2+}$ -vermiculite,  $Na^+$ -saturated vermiculite and  $NH_4^+$ -saturated vermiculite are presented in Figure 1 as curves 1, 2 and 3, respectively. The TG and DTA curves for the  $Mg^{2+}$ -V,  $Na^+$ -V, and  $NH_4^+$ -V are presented in Figure 2 as curves 1, 2 and 3, respectively. The XRD patterns at different temperatures obtained with the high-temperature chamber for  $Mg^{2+}$ -V,  $Na^+$ -V and  $NH_4^+$ -V are included in Figures 3, 4 and 5, respectively.

The dehydration of natural Santa Olalla  $Mg^{2+}$  vermiculite ( $Mg^{2+}$ -V) takes place in two steps, the first one on heating up to  $\sim 125^\circ\text{C}$  and the second one on heating up to 200–250°C, as indicated by DTA/TG (Figure 2, curve 1). X-ray diffraction results (Figure 3) show that a layer separation of 14.4 Å is observed at room temperature. During heating to  $\sim 125^\circ\text{C}$  the layer separation decreased to 11.6 Å. A further decrease to  $\sim 10$  Å occurred at around 200–250°C. These three layer separations are assumed to reflect the presence of two, one and about zero water layers in the interlayer of the vermiculite (Walker, 1956; Walker and Cole, 1957; Keay and Wild, 1961; van Olphen, 1963; Reichenbach, 1994). At low temperatures, the physically adsorbed water, which is not in immediate contact with the  $Mg^{2+}$  ions, leaves the sample. This is indicated by the less pronounced weight loss in the TG curve below 100°C and the small shoulder on the DTA curve below 100°C.

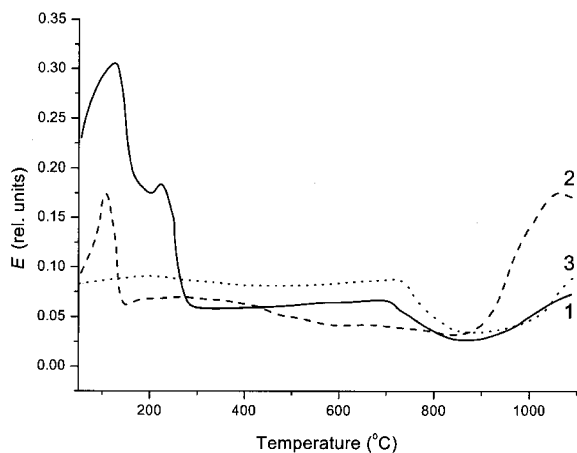


Figure 1. Emanation thermal analysis data of vermiculite samples during heating in air in the temperature range 25–1100°C. Curve 1: initial  $Mg^{2+}$ -vermiculite ( $Mg^{2+}$ -V); Curve 2:  $Na^+$ -vermiculite ( $Na^+$ -V); and Curve 3:  $NH_4^+$ -vermiculite ( $NH_4^+$ -V).

On further heating, water molecules from the first hydration sphere of  $Mg^{2+}$  ions are released. Although the decrease of the layer separation to 11.6 Å normally starts at  $\sim 70^\circ\text{C}$ , the water release continues to a temperature of  $\sim 170^\circ\text{C}$  without further significant change in the layer separation. Around this temperature, the extent of weight loss decreases slightly, the radon release rate reaches its minimum, and the DTA curve

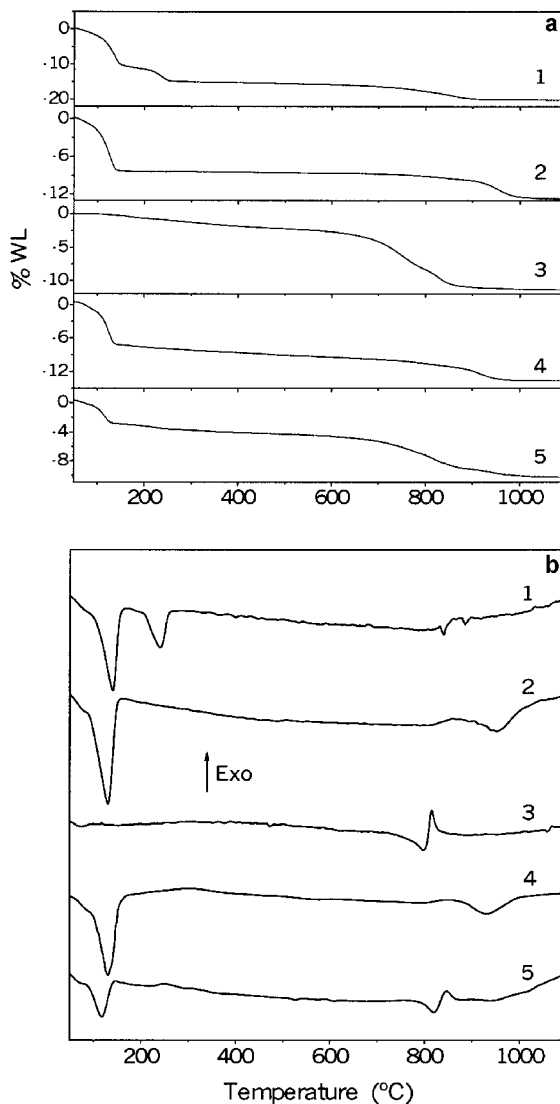


Figure 2. Thermogravimetry (a) and DTA (b) results of vermiculite samples measured during heating in air. (a) TG curves of  $Mg^{2+}$ -vermiculite (curve 1),  $Na^+$ -vermiculite (curve 2),  $NH_4^+$ -vermiculite (curve 3),  $Na^+$ -vermiculite treated with  $(NH_4)_2SiF_6$  totally re-saturated with  $Na^+$  ( $Na^+$ -V<sub>dealum</sub>, curve 4), and  $Na^+$ -vermiculite treated with  $(NH_4)_2SiF_6$  partially re-saturated with  $Na^+$  ( $NH_4^+/Na^+$ -V<sub>dealum</sub>, curve 5). (b) DTA curves of  $Mg^{2+}$ -vermiculite (curve 1),  $Na^+$ -vermiculite (curve 2),  $NH_4^+$ -vermiculite (curve 3),  $Na^+$ -vermiculite treated with  $(NH_4)_2SiF_6$  totally re-saturated with  $Na^+$  ( $Na^+$ -V<sub>dealum</sub>, curve 4), and  $Na^+$ -vermiculite treated with  $(NH_4)_2SiF_6$  partially re-saturated with  $Na^+$  ( $NH_4^+/Na^+$ -V<sub>dealum</sub>, curve 5).

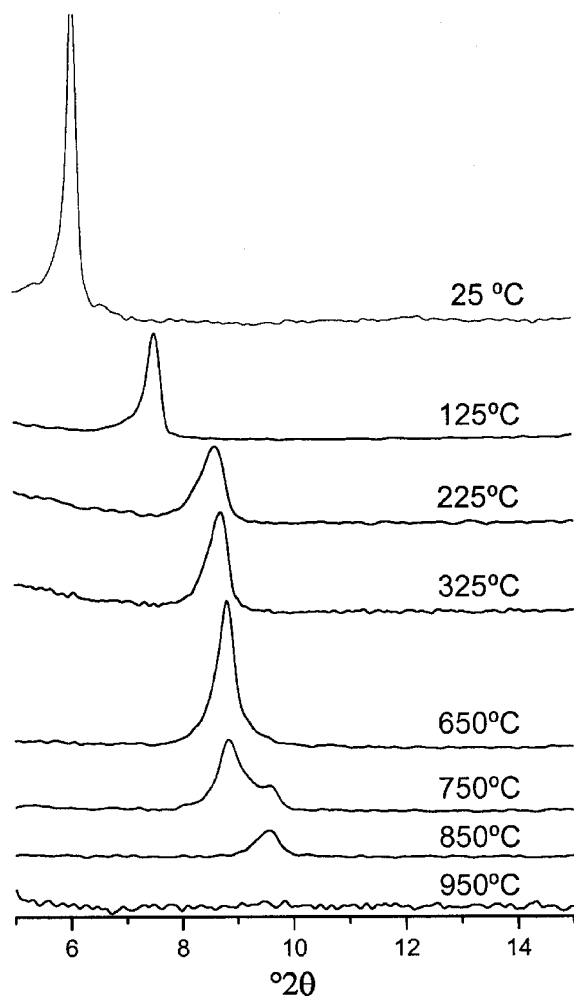


Figure 3. High-temperature XRD patterns of  $\text{Mg}^{2+}$ -vermiculite at different temperatures.

shows no heat flow. The remaining water is lost at 200–250°C, characterized by the additional peak at this temperature in DTA and further weight loss. After this process, nearly unsolvated  $\text{Mg}^{2+}$  ions remain in the vermiculite, indicated by the layer separation of 10 Å, which is only slightly greater than the thickness of the vermiculite layers.

The ETA results clearly support all these observations. Thus, two emanation rate ( $E$ ) increases, one in the range from room temperature to 130°C and the other in the range from 180 to 220°C, followed by sharp decreases in the emanation rate are observed in curve 1, Figure 1. The emanation rate increases are due to the water release in the sample that promotes the emanation of radon. On the other hand, the decreases in the emanation indicate the reduction in the interlayer space and, therefore, the hindering of radon release.

The  $\text{Na}^+$ -V used in this study has a single water layer (layer distance of ~12 Å, Figure 4) because the two-water layer state with a layer distance of 14.8 Å can only be stabilized by soaking the sample in water. The

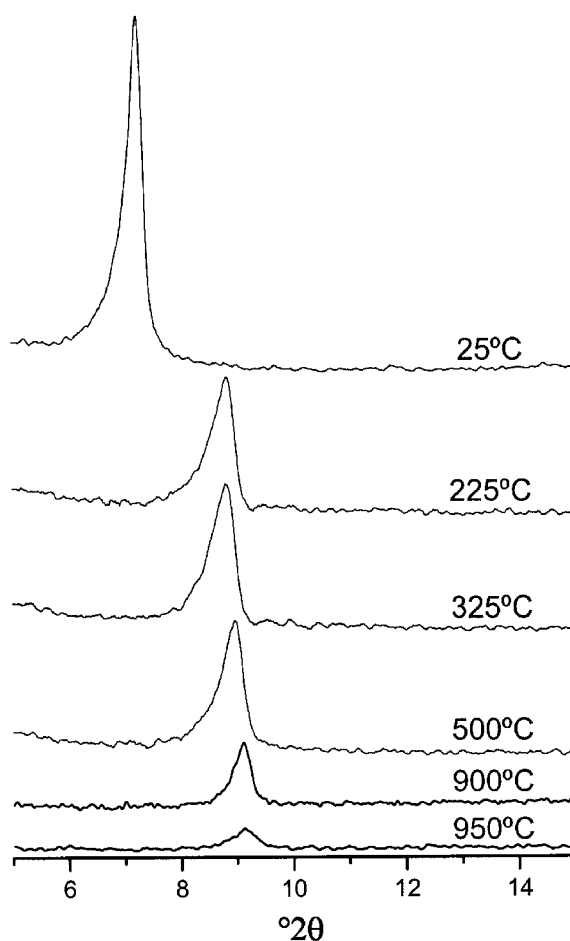


Figure 4. High-temperature XRD patterns of  $\text{Na}^+$ -vermiculite at different temperatures.

dehydration of this sample takes place in one step (Walker and Cole, 1957) as confirmed experimentally in this study by TG and DTA measurements (Figure 2, curve 2). After dehydration, the layer separation is reduced to 9.99 Å, as measured by XRD (Figure 4). The ETA results also showed an increase in the emanation rate during the dehydration of the sample, followed by a sharp decrease in the emanation due to the decrease in the interlayer space.

The  $\text{NH}_4^+$ -V shows a layer separation of ~10.54 Å (Figure 5), indicating that there is nearly no water in the interlayer space and that the ammonium ions may be strongly bound to the silicate layers. The layer distance does not undergo any important change up to 650°C (Figure 5). Thus, it is not surprising that all thermal experiments only show features characteristic of a small water loss in this temperature range (Figure 2, curve 3). Only water in voids and other places may leave the sample as indicated by the continuous slow weight loss in the temperature range from room temperature up to 300°C and the very small increase in radon emanation at ~200°C.

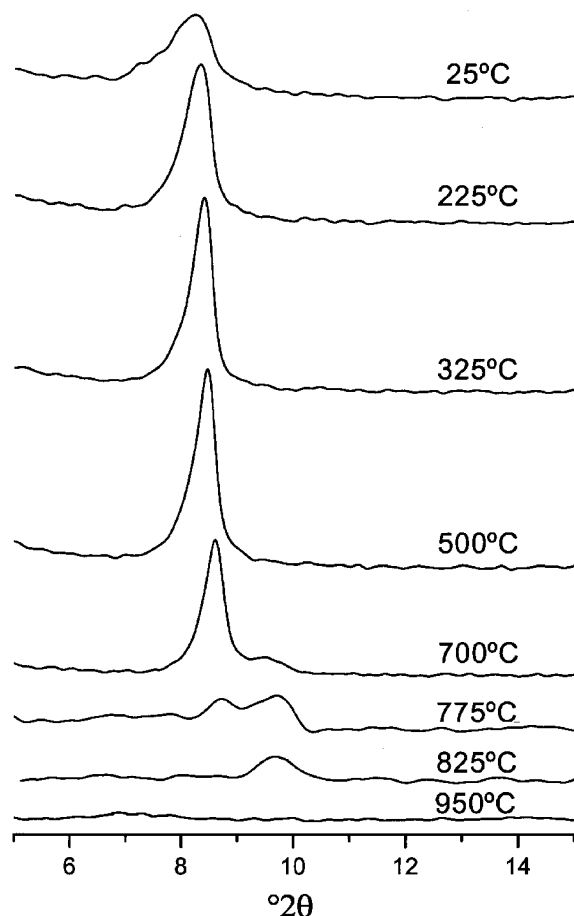


Figure 5. High-temperature XRD patterns of  $\text{NH}_4^+$ -vermiculite at different temperatures.

*Thermal behavior of  $\text{Mg}^{2+}$ -,  $\text{Na}^+$ - and  $\text{NH}_4^+$ -vermiculites in the range 300–1100°C.*

In the temperature range 300–650°C, the ETA curves of all three samples show no significant increase or decrease in the radon release (Figure 1). On the other hand, in the range 650–800°C, decreases in the emanation are observed for the  $\text{Mg}^{2+}$ -V and  $\text{NH}_4^+$ -V samples, while the  $\text{Na}^+$ -V shows no change in the emanation rate in this temperature range. The decreases in the emanation rate for the  $\text{Mg}^{2+}$ -V sample could be attributed to the small decrease of the interlayer space (Figure 3) due to the collapse of the layers produced during the dehydroxylation process recorded by TG at temperatures above 650°C (Figure 2, curve 1). For the  $\text{NH}_4^+$ -V sample, the weight loss in the range 650–900°C (Figure 2, curve 3) is greater (~8.5%) than those due to dehydroxylation of  $\text{Mg}^{2+}$ -V and  $\text{Na}^+$ -V (~4.7%, Figure 2 curves 1 and 2), indicating that both  $\text{H}_2\text{O}$  and  $\text{NH}_3$  are released in this temperature range, as has previously been shown (Pérez-Rodríguez *et al.*, 2001). The decrease in the interlayer space for the  $\text{NH}_4^+$ -V, due to the dehydroxylation and release of ammonia, in the range 650–800°C hinders the diffusion of radon, producing a decrease in the emanation rate of ETA curve (Figure 1,

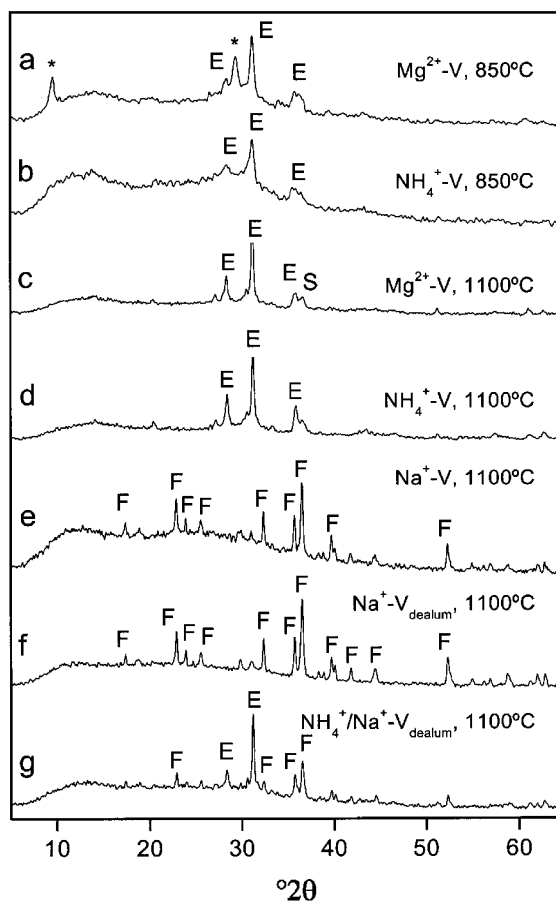


Figure 6. XRD patterns of (a)  $\text{Mg}^{2+}$ -vermiculite heated at 850°C; (b)  $\text{NH}_4^+$ -vermiculite heated at 850°C; (c)  $\text{Mg}^{2+}$ -vermiculite heated at 1100°C; (d)  $\text{NH}_4^+$ -vermiculite heated at 1100°C; (e)  $\text{Na}^+$ -vermiculite heated at 1100°C; (f)  $\text{Na}^+$ - $\text{V}_{\text{dealum}}$  ( $\text{Na}^+$ -vermiculite treated with  $(\text{NH}_4)_2\text{SiF}_6$  and totally re-saturated with  $\text{Na}^+$ ) heated at 1100°C; (g)  $\text{NH}_4^+/\text{Na}^+$ - $\text{V}_{\text{dealum}}$  ( $\text{Na}^+$ -vermiculite treated with  $(\text{NH}_4)_2\text{SiF}_6$  and partially re-saturated with  $\text{Na}^+$ ) heated at 1100°C. E = enstatite; F = forsterite; S = spinel; \* Talc-like phase (Walker and Cole, 1957).

curve 3). On the other hand, for the  $\text{Na}^+$ -V sample, no variation is observed in the interlayer space (Figure 4) during the dehydroxylation process and, therefore, no change is produced in the emanation rate (Figure 1, curve 2).

For the  $\text{Mg}^{2+}$ -V and  $\text{NH}_4^+$ -V samples, heat effects are observed in the DTA curve in the range 800–890°C (Figure 2, curves 1 and 3), and these effects correspond to the crystallization of the vermiculite into new phases. Thus, the XRD patterns of both the  $\text{Mg}^{2+}$ -V and  $\text{NH}_4^+$ -V samples heated to 850°C (Figure 6a,b) show the presence of enstatite. Further heating up to 1100°C produces an increase in the crystallinity of the enstatite phase and a spinel phase is also detected (Figure 6c,d). These increases in the crystallinity of the phases produce an increase in the emanation rate (Figure 1, curves 1 and 3). It has previously been observed (Balek *et al.*, 2002) that crystallization produces a reorganization of atoms

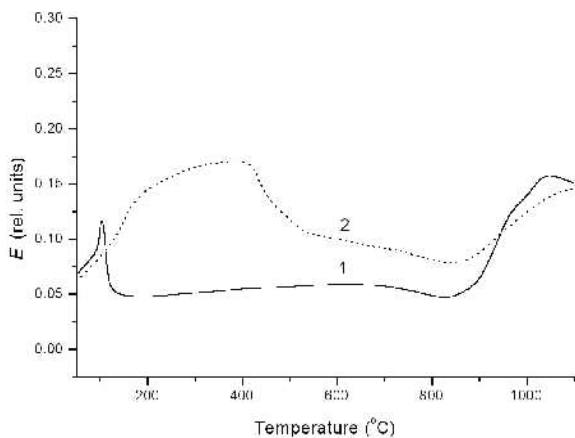


Figure 7. Emanation thermal analysis data of  $(\text{NH}_4)_2\text{SiF}_6$ -treated vermiculites. Curve 1:  $\text{Na}^+$ -vermiculite treated with  $(\text{NH}_4)_2\text{SiF}_6$  and totally saturated with  $\text{Na}^+$  ions ( $\text{Na}^+\text{-V}_{\text{dealum}}$ ). Curve 2:  $\text{Na}^+$ -vermiculite treated with  $(\text{NH}_4)_2\text{SiF}_6$  and partially saturated with  $\text{Na}^+$  ions ( $\text{NH}_4^+/\text{Na}^+\text{-V}_{\text{dealum}}$ ).

into the structure that promotes the formation of new radon diffusion paths in the sample.

For the  $\text{Na}^+\text{-V}$ , the high-temperature weight loss and heat effect take place in a relatively higher temperature range, *i.e.* 850–975°C, than those for the  $\text{Mg}^{2+}\text{-V}$  and  $\text{NH}_4^+\text{-V}$  samples (Figure 2, curve 2). At 1100°C a new phase appears, not seen in  $\text{Mg}^{2+}\text{-V}$  and  $\text{NH}_4^+\text{-V}$ , which can be identified by XRD as forsterite (Figure 6e). Its formation produces a significant increase in radon release (Figure 1, curve 2)

#### Thermal behavior of the $(\text{NH}_4)_2\text{SiF}_6$ -treated vermiculites

Two different samples treated with a  $(\text{NH}_4)_2\text{SiF}_6$  solution have been studied, one of them completely saturated with  $\text{Na}^+$  ions ( $\text{Na}^+\text{-V}_{\text{dealum}}$ ) and the other one partially saturated with  $\text{Na}^+$  ( $\text{NH}_4^+/\text{Na}^+\text{-V}_{\text{dealum}}$ ). The thermal behavior of the  $\text{Na}^+\text{-V}_{\text{dealum}}$  sample (Figure 2, curve 4) does not differ much from that of the  $\text{Na}^+\text{-V}$  sample. Thus, the DTA/TG traces of the  $\text{Na}^+\text{-V}_{\text{dealum}}$  (Figure 2, curve 4) sample are quite similar to that of the  $\text{Na}^+\text{-V}$  sample (Figure 2, curve 2). Additionally, the ETA graph of the  $\text{Na}^+\text{-V}_{\text{dealum}}$  sample (Figure 7, curve 1) is quite similar to that of the  $\text{Na}^+\text{-V}$  (shown in Figure 1, curve 2). The high-temperature XRD pattern of the  $\text{Na}^+\text{-V}_{\text{dealum}}$  (figure not shown) shows identical behavior to that of the  $\text{Na}^+\text{-V}$  sample. These results indicate that, although treatment with a  $(\text{NH}_4)_2\text{SiF}_6$  solution causes (according to d'Espinoze de la Caillerie and Fripiat, 1991) alteration of the vermiculite composition of both tetrahedral and octahedral sheets due to a transfer of Al from the tetrahedral to the octahedral sheets within the structure (the 'translocation' effect), and the partial replacement of Mg by Al in the octahedral sheet, these changes do not produce any modifications of note in the thermal behavior of vermiculite.

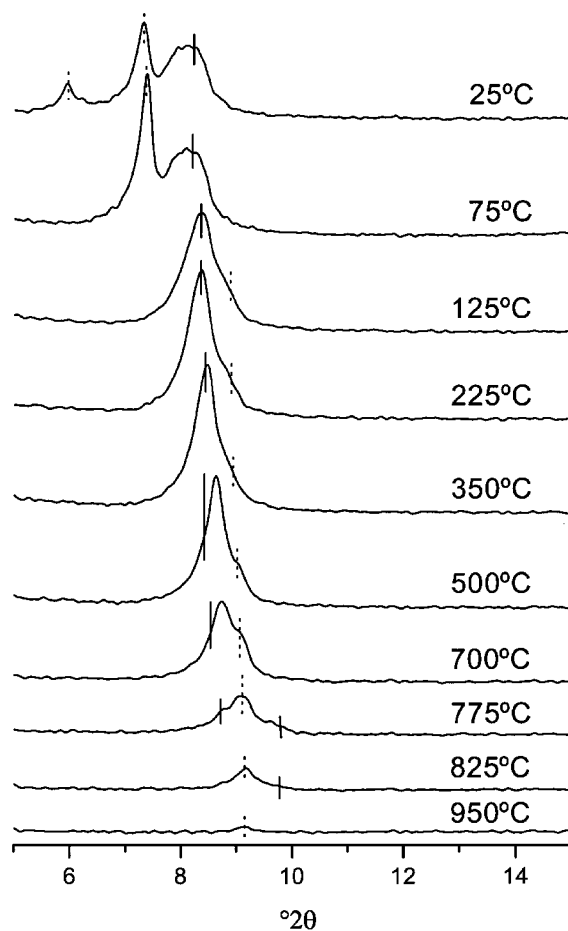


Figure 8. High-temperature XRD patterns of  $\text{Na}^+$ -vermiculite treated with  $(\text{NH}_4)_2\text{SiF}_6$  and partially saturated with  $\text{Na}^+$  ions ( $\text{NH}_4^+/\text{Na}^+\text{-V}_{\text{dealum}}$ ) at different temperatures.

The TG/DTA traces for the sample partially saturated with  $\text{Na}^+$  ( $\text{NH}_4^+/\text{Na}^+\text{-V}_{\text{dealum}}$ , Figure 2, curve 5) are intermediate between those of  $\text{Na}^+\text{-V}$  and  $\text{NH}_4^+\text{-V}$  (Figure 2, curves 2 and 3, respectively). On the other hand, the ETA curve for the  $\text{NH}_4^+/\text{Na}^+\text{-V}_{\text{dealum}}$  (Figure 7, curve 2) sample is very different from those of the  $\text{Na}^+\text{-V}$  and  $\text{NH}_4^+\text{-V}$  samples (Figure 1, curves 2 and 3, respectively). Thus, emanation rate increases from room temperature to  $\sim 375^\circ\text{C}$ . Further heating produces a decrease in the emanation up to  $925^\circ\text{C}$ . Then  $E$  increases again up to  $1100^\circ\text{C}$ .

X-ray diffraction patterns at different temperatures for the  $\text{NH}_4^+/\text{Na}^+\text{-V}_{\text{dealum}}$  sample are included in Figure 8. In addition, the positions of diffraction peaks corresponding to pure  $\text{NH}_4^+\text{-V}$  and  $\text{Na}^+\text{-V}$  phases are marked in the figure as solid and dotted lines, respectively. The sample at room temperature shows diffractions at  $d = 14.8$  and  $12 \text{ \AA}$  that correspond to  $\text{Na}^+$ -vermiculite with two and one water layers, respectively. In addition, a broad peak centered at  $\sim 10.8 \text{ \AA}$  could be attributed to  $\text{NH}_4^+\text{-vermiculite}$ . The IR spectra of this sample (figure not shown) also indicate the presence of



$\text{NH}_4^+$  ions in the interlayer space as indicated by absorption bands at 3270, 3040 and  $1430\text{ cm}^{-1}$  (Chourabi and Fripiat, 1981). For the sample heated to  $75^\circ\text{C}$ , the diffraction at  $d = 14.8\text{ \AA}$  disappears and the intensity of the diffraction at  $12\text{ \AA}$  increases its intensity, indicating that the sample has been partially dehydrated and only one water layer remains. After heating at  $125^\circ\text{C}$ , a diffraction peak at  $d = 10.54\text{ \AA}$  and a shoulder at  $\sim 10\text{ \AA}$  are observed. The peak at  $10.54\text{ \AA}$  could be attributed to the  $\text{NH}_4^+$  in the interlayer space, while the shoulder at  $10\text{ \AA}$  could be attributed to dehydrated  $\text{Na}^+$  in the interlayer space. For temperatures of  $500^\circ\text{C}$  and higher, the position of the peak that was attributed to  $\text{NH}_4^+\text{-V}$  does not match with that of pure  $\text{NH}_4^+\text{-V}$  phase. These experiments seem to indicate that the material does not behave as two segregated phases. To characterize such material, new experimental work and analysis are required; these are outside of the scope of this paper. Nevertheless, it is noteworthy that the onset temperature where the diffraction lines do not correspond with the position of pure  $\text{Na}^+\text{-V}$  and  $\text{NH}_4^+\text{-V}$  is detected in the ETA curve as a decrease in the emanation rate. It is also noteworthy that the  $E$  in the temperature range  $200\text{--}375^\circ\text{C}$  is much higher for the  $\text{NH}_4^+/\text{Na}^+\text{-V}_{\text{dealum}}$  sample than for the  $\text{Na}^+\text{-V}_{\text{dealum}}$  sample, which could be related to the presence of same flakes with both cations in the interlayer. Considering that the cations are of different sizes, diffusion paths could be accessible for the emanation of radon, allowing a greater emanation rate for this sample than for the single-cation samples.

The XRD pattern (Figure 6f) of the fully  $\text{Na}^+$ -saturated sample ( $\text{Na}^+\text{-V}_{\text{dealum}}$ ) heated to  $1100^\circ\text{C}$  is identical to that of the  $\text{Na}^+\text{-V}$  (Figure 6e) heated to the same temperature showing only the presence of forsterite. On the other hand, the XRD pattern of the partially-saturated sample ( $\text{NH}_4^+/\text{Na}^+\text{-V}_{\text{dealum}}$ ) shows a mixture of enstatite and forsterite when heated to  $1100^\circ\text{C}$  (Figure 6g). The first phase is indicative of the presence of some  $\text{NH}_4^+\text{-V}$  in the initial sample. The exclusive formation of forsterite in the case of  $\text{Na}^+\text{-V}_{\text{dealum}}$  and  $\text{Na}^+\text{-V}$  seems to produce more diffusion paths for radon than the simultaneous formation of enstatite and forsterite in the mixed  $\text{NH}_4^+/\text{Na}^+\text{-V}_{\text{dealum}}$  sample, as indicated for a higher emanation rate for the  $\text{Na}^+\text{-V}_{\text{dealum}}$  (Figure 7, curve 1) and  $\text{Na}^+\text{-V}$  samples (Figure 1, curve 2) in the high-temperature range.

## CONCLUSIONS

Emanation thermal analysis (ETA) has been applied for the first time to the characterization of vermiculite using five different samples: natural Santa Olalla  $\text{Mg}^{2+}$ -saturated ( $\text{Mg}^{2+}\text{-V}$ ),  $\text{Na}^+$ -saturated ( $\text{Na}^+\text{-V}$ ),  $\text{NH}_4^+$ -saturated ( $\text{NH}_4^+\text{-V}$ ), chemically treated with  $(\text{NH}_4)_2\text{SiF}_6$  and totally saturated with  $\text{Na}^+$  ( $\text{Na}^+\text{-V}_{\text{dealum}}$ ), and chemically treated with  $(\text{NH}_4)_2\text{SiF}_6$  and partially saturated with  $\text{Na}^+$  ( $\text{NH}_4^+/\text{Na}^+\text{-V}_{\text{dealum}}$ ).

The ETA method is based on the measurement of Rn emanating from the samples and it gives information on microstructural changes in the samples that promote or hinder radon release from the sample. This study has shown that the method is useful for the characterization of the thermal evolution of phyllosilicates. Thus, ETA is very sensitive to changes in the interlayer space. A decrease in the interlayer space hinders the emanation of radon thereby causing a decrease in the emanation rate. For the  $\text{Na}^+\text{-V}$  and  $\text{Mg}^{2+}\text{-V}$  samples, changes in the interlayer space during the dehydration of samples at temperatures below  $300^\circ\text{C}$  have been clearly detected by ETA. Changes in the interlayer space at temperatures  $>300^\circ\text{C}$  for the  $\text{Mg}^{2+}\text{-V}$  and  $\text{NH}_4^+\text{-V}$  samples, were also observed in the ETA curve as a decrease in the emanation rate. For the sample treated with  $(\text{NH}_4)_2\text{SiF}_6$  and completely saturated with  $\text{Na}^+$  ( $\text{Na}^+\text{-V}_{\text{dealum}}$ ), no influence of the dealumination treatment was observed in the thermal behavior of the sample as compared with the  $\text{Na}^+\text{-V}$  sample by conventional and ETA studies. For the sample treated with  $(\text{NH}_4)_2\text{SiF}_6$  and partially saturated with  $\text{Na}^+$  ( $\text{NH}_4^+/\text{Na}^+\text{-V}_{\text{dealum}}$ ), the ETA showed that the material does not behave as two segregated phases, and the presence of two cations affects the thermal behavior of the material.

## ACKNOWLEDGMENTS

This paper is dedicated to the memory of Dr R.C. Mackenzie, pioneer in the use of thermal analysis in the characterization of clay minerals. It was prepared in co-operation between the CSIC and the Academy of Sciences of the Czech republic. This work was supported in part by CICYT through Research Project MAT99-0995 and in part by the Ministry of Education of the Czech Republic, Project No LN00A028. The authors are grateful to Mrs E. Klosova, Nuclear Research Institute, Řež (CZ) for the emanation thermal analysis measurements and to Dr J. Šubrt, IIC, Řež, Czech Republic, for assistance during the preparation of the manuscript. We also thank Dr A. Lurf, Walther-Meißner-Institut, Garching (Germany), for useful discussions and his help in rewriting the manuscript. Suggestions by the referees which helped to improve the manuscript are also cordially acknowledged.

## REFERENCES

- Balek, V. (1989) Characterisation of high-technology materials by Emanation Thermal Analysis. *Journal of Thermal Analysis*, **35**, 405–427.
- Balek, V. (1991) Emanation Thermal Analysis and its application potential. *Thermochimica Acta*, **192**, 1–17.
- Balek, V. and Tölgyessy, J. (1984) Emanation Thermal Analysis and other radiometric emanation methods. In: *Comprehensive Analytical Chemistry*, Vol **12C** (G. Svehla, editor). Elsevier, Amsterdam, 304 pp.
- Balek, V., Malek, Z. and Klosova, E. (1998) Emanation Thermal Analysis of intercalated montmorillonitic clays. *Journal of Thermal Analysis and Calorimetry*, **53**, 625–630.
- Balek, V., Malek, Z., Yariv, S. and Matuschek, G. (1999) Characterization of montmorillonite saturated with various cations. *Journal of Thermal Analysis*, **56**, 67–76.
- Balek, V., Šubrt, J., Mitsuhashi, T., Beckman, I.N. and Györyová, K. (2002) Emanation thermal analysis – Ready

- to fulfil the future needs of materials characterization. *Journal of Thermal Analysis and Calorimetry*, **67**, 15–35.
- Breck, D.W., Blass, H. and Skeels, G.W. (1985) Silicon substituted zeolite compositions and process for preparing same. U.S. Patent **4,503,023**, 27 pp.
- Chourabi, B. and Fripiat, J.J. (1981) Determination of tetrahedral substitutions and interlayer surface heterogeneity from vibrational spectra of ammonium in smectites. *Clays and Clay Minerals*, **29**, 260–268.
- d'Espinose de la Caillerie, J.P. and Fripiat, J.J. (1991) 'Dealumination' and aluminum intercalation of vermiculite. *Clays and Clay Minerals*, **39**, 270–280.
- González-García, F. and García Ramos, G. (1961) Procesos de génesis y degradación de vermiculita. Yacimiento de Santa Olalla (Huelva). III. Génesis de vermiculita. *Anales de Edafología y Agrobiología*, **7–8**, 433–447.
- Justo, A. (1984) Estudio fisicoquímico y mineralógico de vermiculitas de Andalucía y Badajoz. PhD thesis, Universidad de Sevilla, Sevilla, Spain, 408 pp.
- Keay, J. and Wild, A. (1961) Hydration properties of vermiculite. *Clay Minerals Bulletin* **4**, 221–228.
- MacEwan, D.M.C. and Wilson, M.J. (1980) Interlayer and intercalation complexes of clay minerals. Pp. 197–248 in: *Crystal Structures of Clay Minerals and their X-ray Identification* (G.W. Brindley and G. Brown, editors). Monograph **5**, Mineralogical Society, London.
- Malek, Z., Balek, V., Garfinkel-Shweky, D. and Yariv, S. (1997) The study of the dehydration and dehydroxylation of smectites by Emanation Thermal Analysis. *Journal of Thermal Analysis*, **48**, 83–92.
- Miyake, M., Komarneni, S. and Roy, R. (1987) Dealumination of zeolites and clay minerals with  $\text{SiCl}_4$  or  $(\text{NH}_4)_2 \text{SiF}_6$ . *Clay Minerals*, **22**, 367–371.
- Pérez-Maqueda, L.A., Caneo, O.B., Poyato, J. and Pérez-Rodríguez, J.L. (2001) Preparation and characterization of micron and submicron-sized vermiculite. *Physics and Chemistry of Minerals*, **28**, 61–66.
- Pérez Maqueda, L.A., Criado, J.M., Real, C., Balek, V. and Subrt, J. (2002) Emanation Thermal Analysis for characterization of porous hematite under in situ conditions of heating. *Journal of the European Ceramic Society*, **22**, 2277–2281.
- Pérez-Rodríguez, J.L., Poyato, J., Pérez-Maqueda, L.A. and Jiménez de Haro, M.C. (2001) Thermogravimetric and emanation gas analysis of ammonium vermiculite: application to the evaluation of the layer charge. *12<sup>th</sup> International Clay Conference, Bahía Blanca, Argentina*, abstract 107.
- Reichenbach, H. Graf von (1994) Dehydration and rehydration of vermiculites: I Phlogopitic Mg-vermiculite. *Clay Minerals*, **29**, 327–340.
- Van Olphen, H. (1963) Compaction of clay sediments in the range of molecular particle distances. *Clays and Clay Minerals*, **11**, 178–187.
- Walker, G.F. (1956) The mechanism of dehydration of Mg-vermiculite. *Clays and Clay Minerals*, **4**, 101–115.
- Walker, G.F. and Cole, W.F. (1957) The vermiculite minerals. Pp. 191–206 in: *The Differential Thermal Investigation of Clays* (R.C. Mackenzie, editor). Mineralogical Society, London.
- Ziegler, J.F., Biersack, J.P. and Littmark, U. (1985) *The Stopping and Range of Ions in Solids*. Pergamon Press, New York.

(Received 15 August 2000; revised 6 June 2002; Ms. 475; A.E. David A. Laird)